Aggregate Modeling and Coordination of Diverse Energy Resources Under Packetized Energy Management*†

Luis A. Duffaut Espinosa, Mads Almassalkhi, Paul Hines, and Jeff Frolik

Abstract—**Transmitting a large file across the internet requires breaking up the file into smaller packets of data. Packetized energy management (PEM) leverages similar concepts from communication theory to coordinate distributed energy resources by breaking up deferrable residential consumer demands into smaller fixed-duration/fixed-power packets of energy. Each individual load is managed by a probabilistic automaton that stochastically requests energy packets as a function of its local dynamic state (e.g., temperature or state-of-charge). Based on the aggregate request rate from packetized loads and grid conditions, the PEM coordinator will modulate the rate of accepting requests, which permits tight tracking of a reference (load-shaping or market) signal. This paper presents a state bin transition (macro) model suitable for characterizing a diverse population of electric water heaters (EWHs) and energy storage systems (ESSs) under a single PEM coordinator that is validated against a physical micro simulation of the diverse loads. The resulting model provides a measure of real-time flexibility of the aggregate population that is a function of the request rate and illustrate how diversity of packetized load types enhances the level of flexibility offered by the coordinator.**

Index Terms—**Packetized energy management, state bin transition model, controlled Markov chain, distributed energy resources, modeling.**

I. INTRODUCTION

Operating the electric grid reliably with a high penetration of renewable energy represents a significant challenge. To overcome this challenge, an active role for flexible and controllable distributed energy resources (DERs), such as thermostatically-controlled loads (TCLs) and energy storage systems (ESSs) has been proposed [1]. While the core concepts underlying modern demand-side management (DSM) have existed for decades [2], [3], the technology for coordinating the activities of DERs is nascent but maturing rapidly [4]–[6]. This is the context in which PEM aims to contribute as presented in [7], [8].

Under packetized energy management (PEM), a load aggregator requires only the aggregate power consumption and the aggregate request process from a collection of loads to develop control strategies. While aggregate power consumption only informs the system about devices that are ON, PEM's unique packet request process received from the loads that are OFF supplies valuable information about the OFF-population. From this perspective, PEM's limited data requirement represents a significant advantage over other aggregate model-estimator-controller state-space approaches, e.g., [4], which requires an entire histogram of states from the collection of loads to update a state bin transition model. To generate these states for control, an observer

is designed to estimate the histogram based on aggregated power consumption; however, in some cases, the model may not be observable [6].

Recently, the foundational work in [4] has been extended in several directions. For example, higher order dynamic models and end-user compressor delay constraints and lock-out periods have been included in [5], which inspired the modeling of packet duration in PEM presented in this paper. In addition, bounds on stochastic dynamical performance have been developed in [9]. Another approach to achieve direct load control involves mean-field theory applied to heterogeneous TCL populations in [10]. Similarly to the proposed work herein, the mean-field approach developed in [6], [11] maintain quality of service (QoS) by automating opt-out mechanisms and injecting randomization based on local state variables, which limits synchronization effects and promotes equitable access to the grid. However, in contrast to those prior works, PEM does not require to broadcast the control signal (in top-down fashion). Instead, PEM is designed to have each load request an energy packet from the coordinator stochastically (in a locally-driven, bottom-up fashion) based on the load's local state variables. The coordinator then responds in real-time to each packet request based on grid or market conditions.

Furthermore, related work on energy packets is given by [12], [13], where an omniscient centralized *packetized direct load controller* (PDLC) is developed for TCLs. The average controller performance and consumer QoS is analytically investigated and queuing theory is employed by the authors to quantify the centralized controller's performance. In [14], a distributed (binary information) version of PDLC is proposed that requires only (binary) packet request information from the loads. The main drawbacks of the distributed PDLC are that it assumes complete knowledge of the exact number of participating packetized loads at any given time, the allocation of packet requests from the queue is synchronized, and the queue stores packet requests if the packets cannot be allocated, which creates delays in service.

The contributions of this paper includes extending the preliminary macro-model developed for a large population of homogeneous TCLs in [7] and [8] to a *diverse group of DERs*. Specifically, this paper considers TCLs and ESSs in this diverse group. Since an ESS not only consumes power from, but also injects power into the grid, the flexibility provided by an ESS is bidirectional (unlike unidirectional TCLs) and enhances the overall flexibility of the diverse group of loads. Interestingly, the general PEM framework presented herein seamlessly integrates different types of flexible loads, which engenders bottom-up plug-and-play control *across different types of loads* without having to design separate control systems for each load type.

The paper is organized as follows. In Section II, PEM fundamentals are presented. A state bin transition model that models the population dynamics is detailed in Section III.

Section IV combines the population state bin transition model and the PEM abstraction (equivalent to two timers that track energy packets from accepted "consume" and "inject" requests). This is followed by an illustration of how a diverse population of DERs (TCLs and ESSs) under PEM engenders greater flexibility than an all-TCL population.

II. PEM FUNDAMENTALS

PEM is illustrated by the following events:

i. A DER measures its local energy state (e.g., temperature or state of charge).

ii. If the state exceeds some specified limits, the DER exits PEM, reverts to a default DER control until the state is returned to within limits, and returns to Step 1. Else, based on the state, the DER stochastically requests to consume or inject energy from/into the grid for a pre-specified epoch (an energy packet) and goes to Step 3.

iii. The aggregator (or Virtual Power Plant, VPP) either accepts or denies the DER's request, depending on system conditions, such as binding constraints or reference tracking error. If denied, return to Step 1. If accepted, the TCL consumes/inject energy for the epoch and returns to Step 1.

The closed-loop diagram shown in Fig. 1 exercises the rules for PEM control described above.

By employing a probabilistic automata at each responsive load that is capable of exiting PEM to guarantee consumer Quality of Service (QoS), we inject randomization to the load requests based on local state variables, which prevents synchronization, guarantees consumer QoS, and promotes fair access to the grid. Fig. 1 illustrates the closed-loop system under PEM.
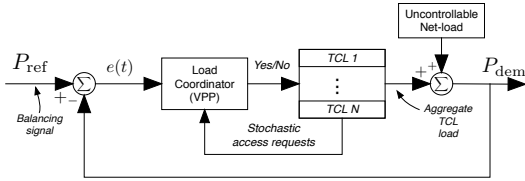

Fig. 1. Closed-loop feedback system for PEM with $P_{\text{ref}}(t)$ provided by the grid or market operator and the aggregate net-load $P_{\text{dem}}(t)$ measured by VPP.

In this paper, the DER load types of interest are EWHs and ESSs. In a population of EWHs, the temperature of EWH n at time t, $T_n(t)$, is

$$\dot{T}_n(t) = \frac{P_n^{\text{rate}} z_n(t)}{c\rho L_n \eta} - \frac{T_n(t) - T_{\text{amb}}}{\tau_n} - \frac{T_n(t) - T_{\text{in}}}{60 L_n} w_n(t) \quad (1)$$

where $\bar{c} = 4.186$ [kJ/kg-°C] and $\rho = 0.990$ [kg/liters] represent specific heat capacity and density of water close to 50°C. L_n [liters] represents the total capacity of the EWH. The input power when ON (i.e., binary $z_n \equiv 1$) is P_n^{rate} [kW], heat-transfer efficiency η is assumed to be 1.0, ambient losses are described by time-constant τ_n, and the uncontrolled hot-water withdrawal rate (i.e., noise) is w_n [liters/min]. The terms T_{amb} and T_{in} are, respectively, the ambient and inlet temperatures [°C], which are considered constant in this paper. The dynamic state variable for ESSs, on the other hand, is the state-of-charge (SOC), The SOC of the n ESS in a population is described by the equation

$$\dot{S}_n(t) = \eta_{\text{sl},n} S_n(t) + \left(z_n(t) P_n^{\text{rate}} + w_n(t) \right) \eta_{z_n,n}(t) \quad (2)$$

where P_n^{rate} is the power rate of the battery, $z_n = 1, 0, -1$ is the hybrid state corresponding to charge/OFF/discharge, respectively, and $\eta_{\text{sl},n}, \eta_{1,n}, \eta_{-1,n}$ represent parameters associated with standing losses and charging/discharging efficiencies, respectively. If standing losses are not considered, $\eta_{\text{sl},n} \equiv 0$. The control inputs are charge and discharge rates [kW], which are each bounded. The SOC is also bounded by battery capacity bounds: $S_n \in \{\underline{S}_n, \overline{S}_n\}$. Finally, the ESS is assumed to be subject to an uncontrollable bounded background net-demand process (charging and/or discharging), $w_n(t) \in [-P_n^{\text{rate}}, P_n^{\text{rate}}]$.

From hereafter, the dynamic state of the nth DER in a population is denoted by the Z_n. In the discrete-time implementation of PEM, the probability that the packetized load n with local dynamic state $Z_n[k] \in [\underline{Z}_n, \overline{Z}_n]$ and desired set-point $Z_n^{\text{set}} \in (\underline{Z}_n, \overline{Z}_n)$ requests access to the grid during time-step k (over interval Δt) is defined by the cumulative exponential distribution function:

$$P(Z_n[k]) := 1 - e^{-\mu(Z_n[k])\Delta t},$$

where the rate parameter $\mu(Z_n[k]) > 0$ is dependent on the local dynamic state. Denoting by $P_k^{\text{h}}(n|Q)$ the probability that load n request a packet for consumption (h = c) or injection (h = d) given condition Q is satisfied. The dependence on the local dynamic state for the probability of request is established by considering the following boundary conditions:

i. $P_k^{\text{c}}(n| Z_n[k] \leq \underline{Z}_n) = 1$, $P_k^{\text{c}}(n| Z_n[k] \geq \overline{Z}_n) = 0$,

ii. $P_k^{\text{d}}(n| Z_n[k] \leq \underline{Z}_n) = 0$, $P_k^{\text{d}}(n| Z_n[k] \geq \overline{Z}_n) = 1$,

which give rise to the following natural design of a PEM rate parameter for *consuming* a packet:

$$\mu(Z_n[k])$$
$$= \begin{cases} 0, & \text{if } Z_n[k] \geq \overline{Z}_n \\ m_R \left(\frac{\overline{Z}_n - Z_n[k]}{Z_n[k] - \underline{Z}_n} \right) \cdot \left(\frac{Z_n^{\text{set}} - \underline{Z}_n}{\overline{Z}_n - Z_n^{\text{set}}} \right), & \text{if } Z_n[k] \in (\underline{Z}_n, \overline{Z}_n) \\ \infty, & \text{if } Z_n[k] \leq \underline{Z}_n \end{cases}$$
$$(3)$$

where $m_R > 0$ [Hz] is a design parameter that defines the mean time-to-request (MTTR). For example, if one desires a MTTR of 5 minutes when $Z_n[k] \equiv Z_n^{\text{set}}$ then $m_R = \frac{1}{600}$ Hz. Similarly, for *injecting* a packet,

$$\mu(Z_n[k])$$
$$= \begin{cases} \infty, & \text{if } Z_n[k] \geq \overline{Z}_n \\ m_R \left(\frac{Z_n[k] - \underline{Z}_n}{\overline{Z}_n - Z_n[k]} \right) \cdot \left(\frac{\overline{Z}_n - Z_n^{\text{set}}}{Z_n^{\text{set}} - \underline{Z}_n} \right), & \text{if } Z_n[k] \in (\underline{Z}_n, \overline{Z}_n) \\ 0, & \text{if } Z_n[k] \leq \underline{Z}_n \end{cases}$$
$$(4)$$

III. STATE TRANSITION UNDER END-USER EVENTS

This section develops a state bin transition (macro)model for a large homogeneous population of DERs *of the same load type*. In particular, the case for TCLs and ESSs are provided for illustration. A generalized macro-model for a diverse population of multiple DER types with charging and discharging is developed; however, a brief preamble is provided on the modeling of end-user events that affect directly the individual DER.

A. Modeling of end-user events

In the case of EWHs and ESSs, end-user events correspond to stochastic water usage and power consumption/production,

respectively. These uncontrollable events can be modeled stochastically by employing a simple birth/death stochastic differential equation for the process, $w_n(t)$. To clarify notation, the subscript n is omitted hereafter as this section focuses on a single DER. Assume that there exists an appropriate probability space $(\Omega, P, \mathcal{F})$, where Ω is the set of events, $\mathcal{F}$ a filtration, and P the probability measure of elements in $\mathcal{F}$. For this purpose, a *Poisson rectangular pulse* (PRP) stochastic differential model is employed [15]. That is,

$$dw(t) = (v(t) - w(t))\, dN_1(t) - w(t)\, dN_2(t), \quad (5)$$

where $v(t)$ is a random variable appropriate for the type of DER under study[1] and N_1 (N_2) is an independent, stationary Poisson point process with constant rate parameter λ_1 (λ_2), representing the initiation (end) of a random end-user event. For an EWH, v describes the hot water usage and can be considered exponentially distributed with mean λ. For an ESS, v may be a symmetric probability density function with mean in a neighborhood of zero given that it must considers positive and negative events.

The aggregate steady state behavior of end-user events is now described. This behavior is employed in the next section to compute the transition probabilities for an aggregated system of DERs in steady state. Denote the expected value of a random process w as $\bar{w}(t) := E[w(t)]$. Due to the independence of the processes ΔN_1, ΔN_2 and v in time, one can compute the expected end-user event for each DER as

$$\frac{d\bar{w}(t)}{dt} = (\bar{v}(t) - \bar{w}(t))\lambda_1 + \bar{w}(t)\lambda_2. \quad (6)$$

The solution of (6) when $w(0) = 0$ is

$$\bar{w}(t) = E[v]\frac{\lambda_1}{\lambda_1 + \lambda_2}(1 - \exp(-(\lambda_1 + \lambda_2)t))$$

The expected event reaches steady state as t goes to infinity. Hence, the steady state end-user event is

$$\bar{w}_{\mathrm{sst}} := \lim_{t \to \infty} \bar{w}(t) = \frac{E[v]\lambda_1}{\lambda_1 + \lambda_2}. \quad (7)$$

The next theorem theorem describes the probability distribution of these events as the number of devices increases. For simplicity, the end-user event are considered as independent and identically distributed random processes.

Theorem 1: The steady state aggregation of individual end-user events, $\bar{w}_{sst}$, is distributed in steady state as $\mathcal{N}(\mu_w, \sigma_w/\sqrt{N_e})$, where N_e is the total number of end-user event processes and μ_w and σ_w are the corresponding expected value and standard deviation of the process w in steady state.

Proof: One can derive the differential equation for the characteristic function of w in (5) from a direct application of the Itô chain rule for jump processes [16]. Let $F_\kappa(w) = e^{i\kappa w}$, then

$$de^{i\kappa w} = (F_\kappa(v) - F_\kappa(w))dN_1 + (1 - F_\kappa(w))dN_2.$$

By definition, the characteristic function of $w(t)$ is $\Psi_w(\kappa, t) = E[F_\kappa(w)]$ and $E(N_i(t)) = \lambda_i(t)$. It then follows that

$$\frac{d\Psi_w(\kappa, t)}{dt} = \Psi_v(\kappa, t)\lambda_1 + \lambda_2 - \Psi_w(\kappa, t)(\lambda_1 + \lambda_2). \quad (8)$$

---

[1]Note that v is independent of N_1 and N_2 and describes the intensity of the end-user event.

In steady state, $\frac{d\Psi_w(\kappa, t)}{dt} = 0$. Thus,

$$\Psi_w(\kappa, \infty) = \frac{\lambda_2 + \Psi_v(\kappa)\lambda_1}{(\lambda_1 + \lambda_2)}.$$

Clearly, the moments of w in steady state can be obtained by computing $E[w^n] = (-i)^n d\Psi_w(\kappa, \infty)/dt|_{\kappa=0}$. A direct application of the central limit theorem for i.i.d random variables completes the proof given that in steady state all end-user events are independent of each other and identically distributed with the distribution associated to the solution of (8). Hence one can consider, on average, that a single DER is driven by a process $\bar{w} \sim \mathcal{N}(\mu_w, \sigma_w)$. ∎

Example 1: If $v \sim \exp(\lambda)$, then

$$\mu_w = \lambda p \ \text{ and } \ \sigma_w = \lambda\sqrt{2p - p^2},$$

where $p := \frac{\lambda_1}{\lambda_1 + \lambda_2}$. □

B. The State Bin Transition Model

For the purpose of constructing a state bin transition macro-model for a large population of DERs, consider the a population whose dynamic states are discretized so that it approaches the behavior of the agent-based micro-model as the number of devices increases [17]. The transition probabilities between bins are determined from the dynamical system equations of the DERs comprising the population. Let $\mathcal{X} = \{x_1, \ldots, x_N\}$, where each element is called a state and constitute a partitioning of the state space Z in which the DERs evolve. Assume that there exists an appropriate probability space $(\Omega, P, \mathcal{F})$, where Ω is the set of events, $\mathcal{F}$ a filtration, and P the probability measure of elements in $\mathcal{F}$. Then, random variables $\{X_k\}_{k \geq 0}$ are defined as $X_k : \Omega \to \mathcal{X}$. Let $x_j \in \mathcal{X}$ and denote $q_j[k] = P(X_k = x_j)$ as the probability of $X_k = x_j$, $k \geq 0$. The column vector $q[k] := (q_1, \ldots, q_N)^T$ then gives the probability mass function of the random variable X_k. Also, if one denotes the transition probability of an homogeneous Markov chain as $p_{ij} = P(X_{k+1} = x_i | X_k = x_j)$, it then follows that

$$q[k + 1] = Mq[k], \quad (9)$$

where $M = \{p_{ij}\}_{1 \leq i, j \leq N}$ [18]. Given an initial distribution $q[0]$, one can solve for (9) and find the distribution at time k as $q[k] = M^k q[0]$.

The focus of this paper is on DERs that have hybrid one dimensional dynamics as in (1) and (2). More specifically, an interval $[Z_{\min}, Z_{\max}]$ within the continuous state space of the DER is divided into N consecutive bins each corresponding to a *bin state* in $\mathcal{X}$. Since (2) includes three types of dynamics (charge/OFF/discharge) and the ON/OFF dynamics of (1) can be seen as charging/OFF dynamics with a disconnected/inaccessible and trivial discharging dynamics, the state space for the system consists of three discrete state spaces: $\mathcal{X}_c$, $\mathcal{X}_{\mathrm{off}}$ and $\mathcal{X}_d$. That is, the full state space is given by $\mathcal{X} = \mathcal{X}_c \cup \mathcal{X}_{\mathrm{off}} \cup \mathcal{X}_d$. At time k, the probability mass function of the system is $q^\top = (q_c^\top, q_{\mathrm{off}}^\top, q_d^\top)$ with $q_c = (q_c^1, \cdots, q_c^N)^\top$ and q_{off} and q_d defined similarly. Note that q contains the percentage of the population in each state of $\mathcal{X}$. For example, if N_e is total number of DERs (coincides with the number of end-user event processes) and $N_{e,c}^i$ is the number of devices in state x_c^i, then $N_{e,c}^i = q_c^i N_e$. Similarly, the percentage of N_e that is charging and discharging, and the total power of the system are

$$y_c = c_c q, \quad y_d = c_d q, \ \text{ and } y = cq, \quad (10)$$

where $c_\text{c} = (\mathbf{1}_N^\top, 0\cdots 0) \in \mathbb{R}^{3N}$, $c_\text{d} = (0\cdots 0, \mathbf{1}_N^\top) \in \mathbb{R}^{3N}$, $c = N_e P^\text{rate}(c_\text{c} - c_d) \in \mathbb{R}^{3N}$, $\mathbf{1}_N = (1, \ldots, 1)^\top \in \mathbb{R}^N$, and P^rate is the average power consumption by the DERs.

Transition rates are computed by considering how the dynamic state interval corresponding to a particular state is altered by the DER hybrid dynamics.
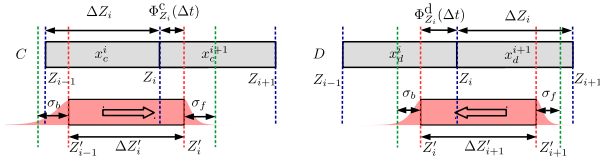

Fig. 2. Transition rates calculation for charging (left) and discharging (right) populations.
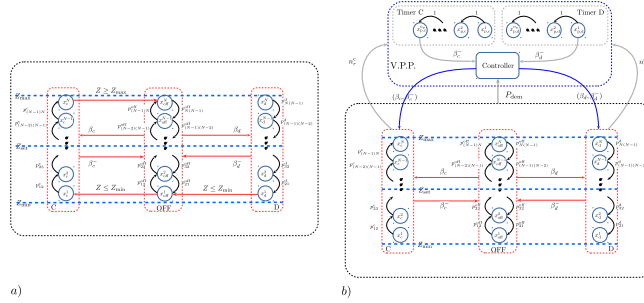

Fig. 3. Abstraction for (a) conventional DER control and (b) PEM control, where self-loops are not visualized.

The main factor affecting these transition rates is the background usage of the DERs by the end-user. However, this usage was modeled in Section III-A as a generic birth and death process known as *Poisson Rectangular Pulse* stochastic differential model [15]. For example, one can simulate the individual water usage by letting the random variable v to be distributed exponentially and fitting the rates of N_1 and N_2 to the average starting and ending of water events [8]. Similarly for an ESS system one can set v to be uniformly (or normally) distributed so that positive/negative values correspond to charging/discharging events.

Thus, the state transition rates for the large population are calculated considering the evolution of (1) and (2) with respect to the average end-user event of the population. The transition rates for the charge/OFF/discharging populations are computed next. Dropping the subscript n in (1) and (2), it follows for EWHs that the solution with steady state end-user event $w = \bar{w}_\text{sst}$ and $T(0) = T_0$ is

$$T(t) = \Phi_{T_0}(t) = e^{-at}\left(T_0 - \frac{b(z)}{a}\right) + \frac{b(z)}{a}, \quad (11)$$

where $a = \frac{1}{\tau} + \frac{\bar{w}_\text{sst}}{60L}$ and $b(z) = \frac{T_{amb}}{\tau} + \frac{T_\text{in}}{60L}\bar{w}_\text{sst} + \frac{P^\text{rate}}{\bar{c}\rho L\eta}z$. For ESSs, since the time-horizon of interest is less than 48 hours, one can set $\eta_\text{ls} \equiv 0$ and, if we assume that v is a zero-mean random variable, one obtains $\bar{w}_\text{sst} = 0$. Making $S(0) = S_0$, one has that

$$S(t) = \Phi_{S_0}(t) = S_0 + \left(z(t)P^\text{rate}\eta_z(t)\right)t. \quad (12)$$

Furthermore, from Theorem 1, one can compute the standard deviation σ_z for (1) and (2) when driven by the stochastic process satisfying $dw = \bar{w}_{sst}\,dt + \sigma_w\,dW(t)$ (W is a standard Wiener process) by solving the following differential equation for the second moment of T and S:

$$\begin{aligned}\dot{\rho}(t) &= (2A(t) + B^2(t))\rho(t) \\ &\quad + 2Z(t)(\alpha(t) + B(t) + \beta(t)) + \beta^2(t),\end{aligned}$$

where $\rho(0) = Z^2(0)$. Then $\sigma_z = \sqrt{\rho - E[Z]^2}$. In particular, EWHs have $A = -1/\tau - \bar{w}_{sst}/(60L)$, $\alpha = zP^{rate}/(\bar{c}\rho L\eta) + T_a/\tau + T_i\bar{w}_{sst}/(60L)$, $B = -\sigma_w/(60L)$ and $\beta = T_i\sigma_w/(60L)$, and ESS have $A = B = 0$, $\alpha = zP^{rate}\eta_z$ and $\beta = \eta_z\sigma_w$. For arbitrary DERs, one can define $\Phi_{Z_0}^\text{c}(t) = \Phi_{Z_0}(t)\big|_{z=1}$, $\Phi_{Z_0}^\text{off}(t) = \Phi_{Z_0}(t)\big|_{z=0}$ and $\Phi_{Z_0}^\text{d}(t) = \Phi_{Z_0}(t)\big|_{z=-1}$. Hereafter, only transitions to adjacent bin states are allowed, which can be implemented by establishing a bound on Δt, as discussed in [8]. The transition probabilities for the charging population, as shown in Fig. 2, are computed by taking the boundaries Z_{i-1} and Z_i corresponding to state x_c^i and computing $Z_{i-1}' = \Phi_{\Delta t}^\text{c}(Z_{i-1})$ and $Z_i' = \Phi_{\Delta t}^Z(Z_i)$. Note that in this case $Z_i < Z_i'$. Thus, the percentage of DERs that remain in x_c^i, move to x_c^{i+1} and move to x_c^{i-1} are, respectively, given by:

$$p_{ii}^\text{c} = \frac{Z_i - Z_{i-1}}{\Delta Z_i' + \sigma_b + \sigma_f}, \quad p_{i(i+1)}^\text{c} = \frac{Z_i' + \sigma_f - Z_i}{\Delta Z_i' + \sigma_b + \sigma_f} \quad \text{and}$$
$$p_{(i-1)i}^\text{c} = 1 - p_{ii}^\text{c} - p_{i(i+1)}^\text{c}.$$

Transition rates for the OFF and discharging dynamics are determined similarly. Note that the DER population does not transition to either a higher temperature (TCLs) or a higher state-of-charge (ESSs) since these represent a higher energy state, and, for $z = 0, -1$, (1) and (2) are driven by non-negative energy losses or zero-mean bounded damping terms. The difference between TCLs and ESSs lies in the choice of σ_b and σ_f. For TCLs, $\sigma_b = 2\sigma_z$ given that this value contains 95% of the distribution mass for the purpose of computing the probabilities of transitioning between adjacent bin states. However, for ESSs, $\sigma_b = 0$ due to the bounds established on the charging rate. In addition, there is the potential for some devices spilling over the right boundary of the interval shown in Fig. 2 (left) when charging. This effect is non-trivial when the end-user events affect the DER dynamics additively fashion, which can be case for ESSs if v is nonzero-mean random variable. Specifically in this paper, it is assumed in Section IV-D that ESSs' have $\eta_\text{ls} = 0$ with no background disturbance (i.e., $\sigma_b = \sigma_f = 0$) in addition to the imposed charging/discharginf power limits. For TCLs, the hot water usage events act multiplicatively via (1) and the spill-over effect to the right of the interval boundary can be ignored ($\sigma_f = 0$).

Assuming conventional hysteretic control of DERs, which is based on keeping the local state variable (e.g., temperature, state-of-charge) within a dead-band $[Z_{min}, Z_{max}]$, one charges a device from the OFF states when $Z \leq Z_\text{min}$, turn OFF discharging devices if $Z \leq Z_\text{min}$ or turn OFF charging devices in the case that $Z \geq Z_{max}$, where $[Z_\text{min}, Z_\text{max}] = [Z_\text{set} - Z_\text{DB}/2, Z_\text{set} + Z_\text{DB}/2]$. The hysteretic control is described in Fig. 3. In the case of a population of DERs consisting only of TCLs, the signals $\beta_\text{c}, \beta_\text{c}^-, \beta_\text{d}$ and β_d^- are always zero and the discharging states are unreachable since TCLs cannot inject power into the grid. In the case of a generic type of DERs, the signals $\beta_\text{c}, \beta_\text{c}^-, \beta_\text{d}$ and β_d^- are user-driven (e.g., ESSs being dispatched by owner or electric vehicles being driven). The state diagram for the Markov chain describing conventional DER control is shown in Fig. 3a. The associated Markov transition matrix M for $\beta_\text{c} = \beta_\text{c}^- = \beta_\text{d} = \beta_\text{d}^- = 0$ is

$$M = \left(\begin{array}{c|c|c} M_\text{c} & M_\text{c,off} & 0_N \\ \hline M_\text{off,c} & M_\text{off} & M_\text{d,off} \\ \hline 0_N & 0_N & M_\text{d} \end{array}\right), \quad (13)$$

where $M_{\rm h}$, for ${\rm h} = \{{\rm c, off, d}\}$, is a tridiagonal matrix containing the probabilities of staying, going to next state and going to the previous state, $M_{\rm c,off} = e_1 e_1^\top p_{\rm c}^{\rm off}$, $M_{\rm off,c} = e_N e_N^\top p_{\rm off}^{\rm c}$, $M_{\rm d,off} = e_N e_N^\top p_{\rm d}^{\rm off}$, e_i denotes the elementary vector with its i-th component equal to 1 and all the others 0, and 0_N denotes the N dimensional zero matrix. Observe that the Markov chain associated to M is irreducible since one can reach any state from any arbitrarily chosen initial state. It follows then that this abstraction possesses a unique invariant distribution since $\mathcal{X}$ is finite dimensional. Nonetheless, the conventional model lacks the flexibility inherent to PEM as discussed in Section II.

IV. PEM BIN MODEL FOR DERS

In this section, PEM is embedded into the Markov model for DERs developed above. Specifically, the state bin model is augmented with a timer comprised of two counters that capture the duration of energy packets being consumed and injected. Finally, additional states are conveniently introduced to account for the opt-out dynamics in order to ensure end-user quality of service (QoS). This permits a virtual power plant (VPP) operator to interact with the DER population through the stochastic packet request mechanism. The VPP regulates the proportion of accepted packet requests (charging and discharging) to allow tight tracking of balancing signals. The developed macro-model compares well with (agent-based) micro-simulations of diverse DERs under PEM and can be represented by a controlled Markov chain. Finally, the paper presents how the aggregate net-demand of TCLs and ESSs under PEM is managed by a single coordinator.

A. PEM Markov Model

Under PEM, a DER can only switch to charging/discharging modes for an epoch if the corresponding charging/discharging packet request is accepted by the VPP coordinator. To capture the unique nature of PEM's fixed packet duration and VPP's role, we leverage prior literature on fault tolerant recovery logic [19] and TCL modeling with compressor lockout periods [5]. In this setting, two *timers* are added to the state bin transition model to track the population with accepted charging/discharging packet requests, respectively. PEM control is decribed as a *controlled Markov chain*.

Definition 1 ([18]): Let $\{u_k\}_{k\geq 0}$ be a sequence of real valued functions taking values on a set U. A Markov chain $\{X_k\}_{k\geq 0}$ is said to be a *controlled Markov chain* (CMC) if its transition matrix $M = M(u) := \{q_{ij}(u)\}_{1 \leq i,j \leq N}$ satisfies

$$P(X_{n+1} = x_{i_{n+1}} | X_n = x_{i_n}, \dots, X_0 = x_{i_0}, u_n, \cdots, u_0)$$
$$= P(X_{n+1} = x_{i_{n+1}} | X_n = x_{i_n}, u_n) = p_{i_{n+1} i_n}(u_n).$$

Note that the resulting matrix $M(u)$ must be a (column) stochastic matrix for any choice of $u \in U$. As usual, the probability mass function of a CMC is computed similarly using $q[k+1] = M(u[k])q[k]$ given an initial distribution $q[0]$ and control policy $u(x)[k] : \mathcal{X} \to U$ for $k = 0, 1, \dots$.

The underlying transition matrix over which PEM is implemented is given by (13), but with $p_{\rm off}^{\rm c} = p_{\rm c}^{\rm off} = p_{\rm d}^{\rm off} = 0$ and $p_{NN}^{\rm c} = p_{11}^{\rm d} = 1$. In this manner the VPP becomes the interface between the three modes of operation.

Suppose $q[k] \in \mathbb{R}^{3N}$ is the probability distribution of the PEM macro-model population at time k, $\beta_{\rm c} = {\rm diag}\{\beta_{\rm c}^1, \dots, \beta_{\rm c}^N\}$ with $\beta_{\rm c}^i \in [0,1]$ the percentage of the OFF-population in state $x_{\rm off}^i$ that is allowed to charge, $\beta_{\rm d} =$ ${\rm diag}\{\beta_{\rm d}^1, \dots, \beta_{\rm d}^N\}$ with $\beta_{\rm d}^i \in [0,1]$ the percentage of the OFF-population in state $x_{\rm off}^i$ that is allowed to discharge, $\beta_{\rm c,off} = {\rm diag}\{\beta_{\rm c,off}^1, \dots, \beta_{\rm c,off}^N\}$ with $\beta_{\rm c,off}^i \in [0,1]$ the percentage of the charging population in state $x_{\rm c}^i$ that is switched OFF, and $\beta_{\rm d,off} = {\rm diag}\{\beta_{\rm d,off}^1, \dots, \beta_{\rm d,off}^N\}$ with $\beta_{\rm d,off}^i \in [0,1]$ the percentage of the discharging population in state $x_{\rm d}^i$ that is switched OFF. The action of instantaneously switching charging, discharging and OFF proportion of devices to a different state in q is given by the transformation:

$$\bar{q}[k] = \bar{M}(\beta_{\rm on}[k], \beta_{\rm off}[k])\, q[k], \tag{14}$$

where $\beta_{\rm on} = (\beta_{\rm c}, \beta_{\rm d})^\top, \beta_{\rm off} = (\beta_{\rm c,off}, \beta_{\rm d,off})^\top$,

$$\bar{M}(\beta_{\rm on}, \beta_{\rm off}) = \begin{pmatrix} I_N - \beta_{\rm c,off} & \beta_{\rm c} & 0_N \\ \beta_{\rm c,off} & I_N - \beta_{\rm c} - \beta_{\rm d} & \beta_{\rm d,off} \\ 0_N & \beta_{\rm d} & I_N - \beta_{\rm d,off} \end{pmatrix}, \tag{15}$$

I_N denotes the N-dimensional identity matrix. Once $\bar{M}(\beta_{\rm on}, \beta_{\rm off})$ has switched some DERs to a new charge/OFF/discharge mode, the matrix M makes the DERs in $\bar{q}$ evolve with the natural dynamics inside each mode of operation. It then follows that

$$q[k+1] = M\bar{M}(\beta_{\rm on}, \beta_{\rm off})q[k]. \tag{16}$$

The next theorem simply says that the sequence $\{X_k\}_{k\geq 0}$ associated to (16) is a CMC.

Theorem 2: Let $\beta_{\rm on}[k], \beta_{\rm off}[k] \in \mathbb{R}^{2N \times N}$ be defined as in (14) $\forall\, k \geq 0$. The sequence $\{X_k\}_{k\geq 0}$ of random variables X_k taking values in $\mathcal{X}$ and probability distribution satisfying (16) is a controlled Markov chain as described by Definition 1 with input $u[k] = (\mathbf{1}_{2N}^\top \beta_{\rm on}[k], \mathbf{1}_{2N}^\top \beta_{\rm off}[k])^\top \in \mathbb{R}^{4N}$.

Proof: The proof is straightforward since matrices in (13) and (15) are stochastic for any $\beta_{\rm on}^i, \beta_{\rm off}^i \in [0,1] \forall i$, and the product of stochastic matrices is a stochastic matrix. ∎

PEM control is based on the notion of charging/discharging requests of the OFF population as a function of their current dynamic bin state (for instance, temperature for TCLs and state-of-charge for ESSs). The number of charging/discharging requests thus are paramount for establishing the limits of PEM and different control strategies under PEM. Define

$$\hat{q}_{\rm h}[k] := \hat{M}_{\rm h} q[k] = {\rm diag}(I_N, T_{\rm req,h}, I_N)\, q[k],$$

where $T_{\rm req,h} = {\rm diag}\{p_1^{\rm req,h}, \dots, p_N^{\rm req,h}\}$, $p_i^{\rm req,h} := 1 - e^{-\mu_{\rm h}(Z_i^m)\Delta t}$ is the request probability assigned to $x_{\rm off}^i$ by (3) with respect to the mid-point of state bin i and ${\rm h} = \{{\rm c, d}\}$. It is obvious that $\hat{q}_{\rm h}$ is not a probability mass function since $\mathbf{1}_N^\top(q_{\rm c} + \hat{q}_{\rm h,off} + q_{\rm d}) < 1$. Note that $\hat{q}_{\rm h} = (q_{\rm c}^\top, \hat{q}_{\rm h,off}^\top, q_{\rm d}^\top)^\top$. Nevertheless the aggregate charge/discharge request rated, i.e., the population that can be switched to charge/discharge, is given by:

$$n_{\rm h}[k] := \mathbf{1}_N^\top \hat{q}_{\rm h,off}[k]. \tag{17}$$

It is assumed that each device cannot, in the same instance, request to both charge and discharge. This implies that if both packet types are requested, they simultaneously cancel each other out and no request is made. Furthermore, for each individual DER, since a charging and a discharging request occur independently: $T_{\rm req,c}$ and $T_{\rm req,d}$ are replaced by

$$T_{\rm req,c\!\!\!/} = T_{\rm req,c}(I_N - T_{\rm req,d}) \text{ and } T_{\rm req,d\!\!\!/} = T_{\rm req,d}(I_N - T_{\rm req,c}),$$

respectively. Thus, under PEM, the VPP determines the rate of accepting charging ($\beta_{\rm c}[k]$) and discharging ($\beta_{\rm d}[k]$) packets. Upon a packet being accepted by the VPP, the DER then

instantly switches to the corresponding state.

The population of devices that switch from OFF to charge/discharge, q^+, is a function of β_c, β_d and q_{off} as

$$q^+[k] := \left(\begin{array}{c|c|c} 0_N & \beta_c[k]T_{req,c,d} & 0_N \\ \hline 0_N & -\beta_c[k]T_{req,c,d} - \beta_d[k]T_{req,d,d} & 0_N \\ \hline 0_N & \beta_d[k]T_{req,d,d} & 0_N \end{array} \right) q[k] = M^+_{\beta_{on}[k]} q[k].$$

Observe that the vector $q^+[k]$ can be partitioned as $q^+[k] = (q_c^+[k], q_{off}^+[k], q_d^+[k])^\top$. The population of DERs that switch from charging/discharging to OFF requires information on the rate of expiring packets. In other words, let δ [secs] be the duration of a packet epoch, then the DERs that have been charging/discharging for δ seconds will turn OFF. A delayed system can be constructed based on the need of keeping track of how many DERs started a packet δ seconds ago. Similar to the preliminary work in [8], two sets of states (timer states) are introduced to the system dynamics to account for the number of charging and discharging DERs, respectively. That is, given δ, the time step Δt, and the two vectors of augmented timer states $x_{p,h} \in \mathbb{R}^{n_p}$ with $n_p = \lfloor \delta/\Delta t \rfloor$ and h = {c, d}, the *timer dynamics* is given by

$$x_{p,h}[k+1] = M_{p,h} x_{p,h}[k] + C_{p,h} q_h^+[k], \quad (18a)$$

where $y_{p,d}[k] = x_{p,h}[k]$, $M_{p,h} \in \mathbb{R}^{n_p \times n_p}$ is a zero matrix except for its first lower diagonal whose components are 1 and $C_{p,h} \in \mathbb{R}^{n_p \times N}$ is responsible for allocating the new charge/discharge population into their corresponding charge/discharge timer states. For DERs that were just switched from OFF to charge, there is a state Z_c such that $\Phi_{Z_c}^c(\delta) = Z_{max}$. Therefore $C_{p,c}$ interrupts packets to prevent exceeding Z_{max}. More precisely, if $Z_{i+1} < Z_c$, $C_{p,c}$ allocates all DERs requesting charging packets from bin $[Z_i, Z_{i+1}]$ into the timer state $x_{p,c}^1$. Otherwise, it allocates DERs with $Z_j > Z_c$ in the timer state $x_{p,c}^j$ with $j = \lfloor (\delta - t_j^c)/\Delta t \rfloor$ and t_j^c the time that the DER takes to move its state from Z_j to Z_{max} – this captures packets that are *interrupted* due to QoS constraints. DERs switching from OFF to discharge similarly define the discharge timer states.

Using the information provided by both timers, one can define the population of DERs that completed their δ-seconds packets (charging and discharging) and therefore turns OFF instantly as

$$q^-[k] := \left(\begin{array}{c|c|c} \beta_c^-[k]I_N & 0_N & 0_N \\ \hline -\beta_c^-[k]I_N & 0_N & -\beta_d^-[k]I_N \\ \hline 0_N & 0_N & \beta_d^-[k]I_N \end{array} \right) q[k] = M_{\beta^-[k]} q[k], \quad (19)$$

where $\beta_h^-[k] := y_{p,h}^{n_p}[k]/(\mathbf{1}_{n_p}^\top y_{p,h}[k])$ with h = {c, d}. The charge/OFF/discharge switching events for the entire population can be formulated as

$$\bar{q}[k] := q[k] + q^+[k] - q^-[k] = (I + M^+_{\beta[k]} - M_{\beta^-[k]})q[k],$$

which yields the DER population dynamics:

$$q[k+1] = M(I + M^+_{\beta[k]} - M_{\beta^-[k]})q[k]$$
$$= \bar{M}(\beta_{on}[k], \beta_{off}[k])q[k], \quad (20)$$

where $\beta_{on}[k] = (\beta_c[k]T_{req,c,d}, \beta_d[k]T_{req,d,d})^\top$ and $\beta_{off}[k] = (\beta_c^- I_N, \beta_d^- I_N)^\top$. Observe that, as in [8], that there is no order in which DERs are switched to charge, OFF or discharge since this events happen instantaneously and simultaneously every Δt seconds. Fig. 3b shows the state diagram of the population model under PEM control.

From Theorem 2, the following corollary follows directly.

Corollary 1: The sequence $\{X_k\}_{k \geq 0}$ of random variables

X_k taking values in $\mathcal{X}$ and probability distribution satisfying (20) is a controlled Markov chain with input $u[k] = \left(\mathbf{1}_N^\top \beta_c[k]T_{req,c,d}, \mathbf{1}_N^\top \beta_d[k]T_{req,d,d}, \mathbf{1}_N^\top \beta_c^- I_N, \mathbf{1}_N^\top \beta_d^- I_N \right)^\top$.
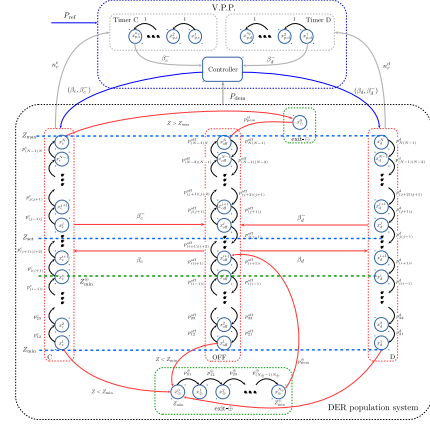

Fig. 4. PEM macromodel with exit-ON ($\oplus$) dynamics. ON/OFF state transitions are controlled by VPP and illustrated with gray and blue arrows. In the case of different classes of DERs (i.e., having several sets of bin states for each DER class), the VPP receives all c/d requests regardless of which population they are from.

Another advantage of the PEM approach is that every OFF DER's charge/discharge request may include its rated value P^{rate_n}. This information does not violate the privacy agreement between each device and the coordinator (as it does not provide the DER's dynamic state) and overcomes the challenge of estimating the rated value from the aggregate power output. Importantly, this renders the system observable in the sense that the coordinator can estimate the population in each bin[2].

B. Tracking with PEM DER Macromodel

Under PEM, the inputs β_c and β_d are exogenous and produced exclusively by the VPP. Recall that, at each instant of time k and for each class of request (charge or discharge), every request is sent with its corresponding $P_n^{rate,h}$ value, which imply that $P^{rate,h} := \frac{1}{n} \sum_{n=1}^{\beta_h n_h} P_n^{rate,h}$ for h = {c, d}. Also, let P_{ref} be the VPP's reference power signal provided by grid or market operator and let P_{dem} be the aggregate net-demand of the diverse packetized DERs measured by the VPP. In particular,

$$P_{dem}[k] := P_c[k] - P_d[k] - P_{OFF,c}[k] + P_{OFF,d}[k],$$

where $P_c[k]$ is the power drawn by all DERs that consume power when charging, $P_d[k]$ is the power injected by all DERs that discharge power into the system, $P_{OFF,c}[k]$ is the power that DERs stop consuming after these were charging at time $k-1$ and subsequently were switched OFF at time k and $P_{OFF,d}(k)$ is the power that DERs stop injecting after these were discharging at time $k-1$ and subsequently were switched OFF at time k. Given n_c and n_d in (17) and that PEM tracking is activated as in Fig. 1, the inputs $\beta_c[k]$ and $\beta_d[k]$ in Fig. 3b are generated by the VPP to minimize tracking error, so that n_c and n_d are maximized at each

---

[2]Due to space constraints, observability results on the PEM Markov model are omitted, but are based on the concepts for bilinear systems [20] and the Popov-Belevitch-Hautus test for time-varying linear systems in [21].

k (to maximize QoS). That is, one solves the following optimization problem:

$$\max_{\xi[k],\nu[k]} \quad \xi[k] + \nu[k] \quad \text{subject to}$$

$$\xi[k]\, P^{\text{rate,c}}[k] + \nu[k]\, P^{\text{rate,d}}[k] = P_{\text{error}}[k],$$
$$0 \leq \xi[k] \leq n_c, \quad 0 \leq \nu[k] \leq n_d.$$

where $P_{\text{error}} = P_{\text{ref}}[k] - P_{\text{dem}}[k]$ is the VPP tracking error and $n_c[k]$ ($n_d[k]$) is the VPP's total number of charging (discharging) requests received at k.

Example 2: Assuming $P^{\text{rate,c}}[k] \approx P^{\text{rate,d}}[k] =: P^{\text{rate}}[k]$, one has that if $P_{\text{error}}[k] > 0$ and $P_{\text{c,d}}[k] := \min\{n_c[k]P^{\text{rate}}[k] - P_{\text{error}}[k], n_d[k]P^{\text{rate}}[k]\}$

$$\xi[k] = \begin{cases} (P_{\text{error}}[k] + P_{\text{c,d}}[k])/P^{\text{rate}}[k], & n_c[k] > P_{\text{error}}[k], \\ n_c[k], & n_c[k] < P_{\text{error}}[k], \end{cases}$$

$$\nu[k] = \begin{cases} P_{\text{c,d}}[k])/P^{\text{rate}}[k], & n_c[k] > P_{\text{error}}[k], \\ 0, & n_c[k] < P_{\text{error}}[k], \end{cases}$$

and when $P_{\text{error}}[k] < 0$ and $P_{\text{d,c}}[k] := \min\{n_c[k]P^{\text{rate}}[k], n_d[k]P^{\text{rate}}[k] - |P_{\text{error}}[k]|\}$

$$\xi[k] = \begin{cases} P_{\text{d,c}}[k])/P^{\text{rate}}[k], & n_d[k] > |P_{\text{error}}[k]|, \\ 0, & n_d[k] < |P_{\text{error}}[k]|, \end{cases}$$

$$\nu[k] = \begin{cases} (|P_{\text{error}}[k]| + P_{\text{d,c}}[k])/P^{\text{rate}}[k], & n_d[k] > |P_{\text{error}}[k]|, \\ n_d[k], & n_d[k] < |P_{\text{error}}[k]|. \end{cases}$$

$\square$

One can observe that if $\beta_{\text{c}}[k] = \beta_{\text{d}}[k] = 0$ for all k then the state diagram in Fig. 3b becomes reducible since, after the first n_p time instants, states are not able to leave their current state class (charge, OFF or discharge states). This causes states in the three classes to become absorbent for $k \to \infty$. Additional states are added in a manner that DERs charge even when the VPP sets $\beta_{\text{c}}[k] = 0$. This *exit-$\oplus$* mechanism is augmented to the PEM macro-model to ensure QoS as described next.

The last item in this section involves quantifying the one step ahead flexibility provided by PEM. One step ahead flexibility in this context is defined as the maximum amount of power that the population system can increase or decrease in the next time instant. Two types of flexibility can be introduced: upward flexibility and downward flexibility. These quantities are defined by the following formulas:

$$\overline{flex}[k] = (n_{\text{c}}[k] - n_{\text{off,c}}[k])P^{\text{rate,c}} + n_{\text{off,d}}[k]P^{\text{rate,d}}. \quad (21a)$$

$$\underline{flex}[k] = (n_{\text{d}}[k] + n_{\text{off,d}}[k])P^{\text{rate,d}} - n_{\text{off,c}}[k]P^{\text{rate,c}}$$
$$+ n_{\text{exit-}\oplus}[k](P^{\text{rate,c}} + P^{\text{rate,d}})/2, \quad (21b)$$

where $n_{\text{off,c}}$ and $n_{\text{off,d}}$ are, respectively, the number of expiring charging and discharging packets (including interruptions) and $n_{\text{exit-}\oplus}$ is the number of devices leaving exit-$\oplus$ mode. These expressions tell the amount of power that the VPP has available for tracking a signal above and below the current output power of the population system.

C. Exit-$\oplus/\ominus$ Dynamics

The end-consumer's QoS is of paramount importance in any large-scale DER coordination scheme such as PEM. Therefore, when a DER's dynamic state falls outside its pre-determined "comfort-zone" or dead-band $[Z_{min}, Z_{max}]$, the device automatically opts out of PEM's requesting scheme
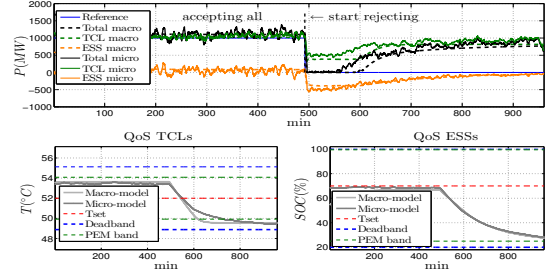

Fig. 5. Validating the homogeneous macromodel by comparing the aggregate power (top) and internal average temperature (bottom) against those of a homogeneous microsimulation with $N = 1000$ packetized electric water heaters.

and, instead, enters *exit-$\oplus$*, which temporarily reverts the device to conventional control that drives the device's state back to within a pre-specified PEM opt-in interval. Once the *exit-$\oplus$*'s set-point is reached, the DER re-enters PEM's energy packet request scheme.

The population of DERs that exit PEM when $Z < Z_{\min}$ join the *exit-$\oplus$* mode dynamics. On the other hand if the DER is such that $Z \geq Z_{\max}$ then it turns OFF by briefly joining the trivial *exit-$\ominus$* mode dynamics at state $x_{\ominus}^0$ after which the DERs transition naturally under M to the charging/discharging requesting states. In Section II, these two modes of operation were briefly discussed for the agent based scheme simulation. Fig. 4 shows the exit-$\oplus/\ominus$ states acting on the PEM scheme. The transition rates are computed in the exact same manner described in Section III-B. In the same figure, $Z_{\min}^{\oplus} = Z_{\text{set}} - Z_{\text{PEM}}$. It then follows that the updated full population dynamics for DERs under PEM are given by (18) together with:

$$q[k+1] = M_{\text{exit}}(I + M_{\beta[k]}^{+} + M_{\beta^{-}[k]}^{-})q[k], \quad y[k] = c^{\top}q[k],$$

where $M_{\text{exit}} := \text{diag}\{M_{\text{exit-}\oplus}, \bar{M}, M_{\text{exit-}\ominus}\}$, $M_{\text{exit-}\oplus}$ is a matrix of zeros except for the main diagonal $(p_{11}^{\oplus}, \ldots, p_{N_{\oplus}N_{\oplus}}^{\oplus})$ and the first lower and upper diagonals which respectively are $(p_{12}^{\oplus}, p_{23}^{\oplus} \ldots, p_{(N_{\oplus}-1)N_{\oplus}}^{\oplus})$ and $(p_{21}^{\oplus}, p_{32}^{\oplus} \ldots, p_{N_{\oplus}(N_{\oplus}-1)}^{\oplus})$, $M_{\text{exit-}\ominus}$ introduces the probabilities to re-enter PEM from $x_{\ominus}^N$ to $x_{\ominus}^0$ and from $x_{\ominus}^0$ to x_{off}^N with $p_{\text{pem}}^{\ominus}$ corresponding to the *exit-$\ominus$* mode, and $\bar{M}$ is such that $\bar{M}_{ij} = M_{ij}$ except for $M_{(N+N_{\oplus}+1)N_{\oplus}} = p_{\text{pem}}^{\oplus}$, which describe the transition probabilities to re-enter PEM from the *exit-$\oplus$* mode.

D. Diverse Macromodel and Validation

Two illustrative simulations are presented in this section, one compares the macro-model provided in the previous section against the agent based simulation (micro-model) for a mixed DER population of 1000 EWHs and 300 ESSs (using the specifications of the homogeneous Tesla Powerwall 2.0) in which all charging/discharging packets ($\beta^{\text{c}} = \beta^{\text{d}} = 1$) are accepted followed by suddenly rejecting all charging/discharging packets ($\beta^{\text{c}} = \beta^{\text{d}} = 0$). And the other compares the simulation of a homogeneous TCL-only VPP of 1300 EWHs tracking a random signal against that of a diverse VPP of 1000 EWHs and 300 ESSs tracking the same random signal. Both simulations are performed over a 16 hour period with $\Delta t = 15$ seconds and where all the DERs had their charge/discharge 5 minute packets accepted for the first 8.8 hours. The homogeneous TCLs
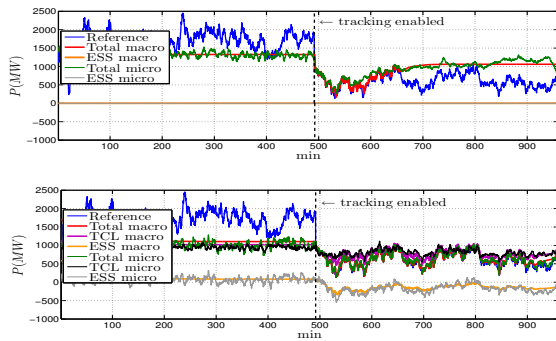
Fig. 6. (Top) Homogeneous macro/micro-model simulation of 1300 TCLs tracking a random signal and (Bottom) Diverse population of 1000 TCLs and 300 ESSs tracking the same random signal under one VPP.

in this study had a set temperature of $52°C$ inside the deadband $[45.75, 58.24]°C$ with PEM lower bound equal to $47.84°C$. The homogeneous ESSs, on the other hand, have SOC set point of $70\%SOC$ inside the dead-band interval $[20, 100]\%SOC$ with PEM lower bound of $25\%SOC$. To validate the macro-model's performance, it is compared against a diverse (agent-based) PEM micro-model simulation similar to [22]. It is shown through simulation that the mean behavior of the macro-model compares well with the micro-model simulation.

Figure 5 shows the result of the first experiment. Clearly, the "accepting all" steady state macro and micro-model simulations agree (modulo the stochastic variability of the micro-model). Still the error between steady state behaviors of macro and micro-model simulations during period of accepting all charge/discharge requests are within a reasonable $\pm 5\%$ of the nominal power value. A similar outcome is observed for the error between steady state behaviors of macro and micro-model simulations during the period of rejecting all charge/discharge requests. The main difference between macro and micro-model simulations is in the speed at which the TCL population reaches steady state behavior after start rejecting all packet requests. This is mainly due to large end-user events for EWHs whose temperature is very close to the lower boundary of the deadband, which results into a very small number of devices exiting PEM regardless of the aggregated temperature of the system. The same effect is reflected in the QoS for TCLs whereas ESSs do not present such issue.

The result of the second experiment is given in Fig. 6. In the top part of the figure, a homogeneous TCL population is trying to track a random signal. However, the system fails due to QoS constraints. Specifically, the system is unable to track the random power reference signal since $n_d = n_{\text{off,d}} = 0$ in (21a) and (21b). From Fig. 6 and (21b), the exit-$\oplus$ population dominates after minute 660 and the 1300 HWHs offer no downward flexibility, which affects the TCL-only VPP's ability to track the random signal. On the other hand, by adding bidirectional DERs (i.e., ESSs) with TCLs to PEM, the downward flexibility in (21b) increases due to discharging requests, which improves the ability of the VPP to track the random signal. Note that the effect of adding ESSs into the PEM game does not decrease the upward flexibility, since ESSs can charge too. Thus, diversity in the

population is enabled seamlessly by PEM without having to modify the automata logic at the load or the VPP control mechanism. Clearly, the performance of the diverse VPP is superior. Due to space constraints additional comparisons are omitted, however, the root mean square error between macro and micro-model aggregated dynamic states for the diverse VPP amounts to less than $0.8°C$ for the TCLs and less than 5.0% SOC for the ESSs while tracking the random signal.

References

[1] D. S. Callaway and I. A. Hiskens, "Achieving Controllability of Electric Loads," *Proceedings of the IEEE*, vol. 99, no. 1, pp. 184–199, Jan. 2011.

[2] M. Morgan and S. Talukdar, "Electric power load management: Some technical, economic, regulatory and social issues," *Proceedings of the IEEE*, vol. 67, no. 2, pp. 241 – 312, 1979.

[3] F. C. Schweppe, R. D. Tabors, J. L. Kirtley, H. R. Outhred, F. H. Pickel, and A. J. Cox, "Homeostatic utility control," *IEEE Trans. Power Apparatus and Systems*, no. 3, pp. 1151–1163, 1980.

[4] J. L. Mathieu, S. Koch, and D. S. Callaway, "State Estimation and Control of Electric Loads to Manage Real-Time Energy Imbalance," *IEEE Transactions on Power Systems*, vol. 28, no. 1, pp. 430–440, 2013.

[5] W. Zhang, J. Lian, C.-Y. Chang, and K. Kalsi, "Aggregated Modeling and Control of Air Conditioning Loads for Demand Response," *IEEE Transactions on Power Systems*, vol. 28, no. 4, pp. 4655–4664, 2013.

[6] Y. Chen, A. Busic, and S. P. Meyn, "State estimation and mean field control with application to demand dispatch," in *2015 54th IEEE Conference on Decision and Control*. IEEE, Dec. 2015, pp. 6548–6555.

[7] M. Almassalkhi, J. Frolik, and P. Hines, "Packetized energy management: asynchronous and anonymous coordination of thermostatically controlled loads," *IEEE American Control Conference*, May 2017.

[8] L. Duffaut Espinosa, M. Almassalkhi, P. Hines, S. Heydari, and J. Frolik, "Towards a Macromodel for Packetized Energy Management of Resistive Water Heaters," *IEEE Conference on Information Sciences and Systems*, March 2017.

[9] S. Esmaeil Zadeh Soudjani and A. Abate, "Aggregation and Control of Populations of Thermostatically Controlled Loads by Formal Abstractions," *IEEE Transactions on Control Systems Technology*, vol. 23, no. 3, pp. 975–990, May 2015.

[10] N. Mahdavi, J. Braslavsky, and C. Perfumo, "Mapping the Effect of Ambient Temperature on the Power Demand of Populations of Air Conditioners," *IEEE Transactions on Smart Grid*, vol. 99, pp. 1–11, Jul. 2016.

[11] S. P. Meyn, P. Barooah, A. Busic, Y. Chen, and J. Ehren, "Ancillary Service to the Grid Using Intelligent Deferrable Loads," *IEEE Transactions on Automatic Control*, vol. 60, no. 11, pp. 2847–2862, Nov. 2015.

[12] B. Zhang and J. Baillieul, "A packetized direct load control mechanism for demand side management," in *IEEE Conference on Decision and Control*, 2012, pp. 3658–3665.

[13] B. Zhang and J. baillieul, "A novel packet switching framework with binary information in demand side management," in *IEEE Conference on Decision and Control*. IEEE, 2013, pp. 4957–4963.

[14] B. Zhang and J. Baillieul, "Control and Communication Protocols Based on Packetized Direct Load Control in Smart Building Micro-grids," *Proceedings of the IEEE*, vol. 104, no. 4, pp. 837–857, 2016.

[15] S. G. Buchberger and L. Wu, "Model for instantaneous residential water demands," *Journal of Hydraulic Engineering*, 1995.

[16] P. E. Protter, *Stochastic Integration and Differential Equations*. Berlin: Springer, 2005.

[17] N. Lu and D. P. Chassin, "A state-queueing model of thermostatically controlled appliances," *IEEE Transactions on Power Systems*, vol. 19, no. 3, pp. 1666–1673, Aug. 2004.

[18] P. R. Kumar and P. Varaiya, *Stochastic Systems: Estimation, Identification and Adaptive Control*. Prentice Hall, 1986.

[19] H. Zhang, W. S. Gray, and O. R. Gonzalez, "Performance Analysis of Digital Flight Control Systems With Rollback Error Recovery Subject to Simulated Neutron-Induced Upsets," *IEEE Transactions on Control Systems Technology*, vol. 16, no. 1, pp. 46–59, 2008.

[20] G. C. Goodwin and K. S. Sin, *Adaptive filtering prediction and control*. Englewood Cliffs, NJ: Prentice-Hall Inc, 1984.

[21] E. I. Verriest, "On balanced realizations for time varying linear systems," Ph.D. dissertation, Stanford University, 1980.

[22] R. M. Hermans, M. Almassalkhi, and I. A. Hiskens, "Incentive-based Coordinated Charging Control of Plug-in Electric Vehicles at the Distribution-transformer Level," *IEEE American Control Conference*, pp. 264–269, Jun. 2012.